Polymeric Foams from High-Performance Thermoplastics

L. SORRENTINO
CNR–Institute for Composite and Biomedical Materials, P. le Tecchio 80, 80125 Naples, Italy

IMAST–Technological District on Polymeric and Composite Materials Engineering and Structures, P.le E. Fermi 1, località Porto del Granatello, 80055 Portici, Naples, Italy

M. AURILIA
IMAST–Technological District on Polymeric and Composite Materials Engineering and Structures, P.le E. Fermi 1, località Porto del Granatello, 80055 Portici, Naples, Italy

S. IANNACE
CNR–Institute for Composite and Biomedical Materials, P.le Tecchio 80, 80125 Naples, Italy

IMAST–Technological District on Polymeric and Composite Materials Engineering and Structures, P.le E. Fermi 1, località Porto del Granatello, 80055 Portici, Naples, Italy

Received: May 7, 2010
Accepted: January 16, 2011

ABSTRACT: The aim of this work was to investigate the foaming process of high-performance thermoplastic polymers such as polyethersulfone (PES), polyphenylsulfone (PPSU), polyetherimide (PEI), and poly(ethylene-2,6-naphthalate) (PEN) expanded by using supercritical carbon dioxide as a blowing agent. All polymers were characterized by differential

Correspondence to: L. Sorrentino; e-mail: luigi.sorrentino@cnr.it.
Contract grant sponsor: MIUR (Italy) within the FIRB project "MANTA"
Contract grant number: RBIP065YCL.

scanning calorimetry (DSC) and rheological analysis to roughly identify the foaming conditions. Batch and solid-state foaming methods were employed. In the first case, cell nucleation was promoted by inducing a fast pressure drop rate in a pressurized vessel. In the solid-state process, foaming was promoted by increasing the temperature of gas-saturated samples in an oil bath. The effects of foaming methods and process parameters on cellular morphology were analyzed. All polymers were successfully foamed by using the solid-state technique, showing relative densities ranging from 0.13 to 0.44 for PEN and from 0.27 to 0.57 for PES, PPSU, and PEI. The morphology was microcellular in all cases, and PES exhibited nanocellular cells after some processing conditions. The batch-foaming process was less effective to prepare foams than the solid-state one. In fact, higher relative densities and reduced temperature windows for foaming were evidenced for amorphous polymers, whereas PEN crystallized during the heating step and foams with poor morphology and high relative densities were obtained. Adv Polym Techn 30: 234–243, 2011; View this article online at wileyonlinelibrary.com. DOI 10.1002/adv.20219

KEY WORDS: Batch foaming, Foams, High-performance polymers, Morphology, Solid state foaming

Introduction

The growing need of decreasing weight in high-performance applications such as in automotive, transport, and aeronautic industries is increasing the use of foams in lightweight structures when high bend and shear strength, high rigidity, good impact strength, low thermal, acoustic, and electric conductivity are required. Conventionally, polymeric foams are employed in many applications such as packaging, thermal and acoustic insulation, and in absorption of impact energy. The service temperature of these conventional applications is not much different from the room temperature,[1] but one of the new main requirements in high-performance applications is the availability of foams capable of being continuously used at high temperatures.[2–4]

To maximize the mechanical properties after the linear elastic region, a microcellular (cell density of at least 10^9 cells/cm^3 and diameters of less than 10 μm should be prepared[5–7]) closed-cell structure in foams should be produced. Today, very few high-performance microcellular foams are available in the market, probably due to the difficulties in manufacturing them. They are based on thermosetting polymers and are usually obtained by using complex and long processes, such as foaming from low molecular weight precursors[8] or stabilizing the cellular structure by means of polymer cross-linking.[9]

Owing to their several advantages over the thermosetting polymers (recyclability, weldability, reduced processing time, and lower manpower), thermoplastics are preferred but a complete understanding of foamability conditions of high-performance thermoplastic matrices is still lacking.

The main procedure used for the production of thermoplastic polymeric foams is based on the following steps: (a) solubilization of the blowing agent (usually a gas) in the polymer, (b) generation of a thermodynamic instability in the solution (through a pressure drop or a temperature increase) to induce cell nucleation and growth, and (c) stabilization of the cellular structure by means of a cooling step.[10] The morphology and the relative density of foams are significantly influenced by the blowing agent solubility, saturation pressure, foaming time, foaming temperature, and pressure drop rate, so the microstructure can be tailored through the careful choice of the foaming conditions to produce a wide range of foam densities and cellular morphologies.[3–5]

To better understand the foaming process of polymers, discontinuous processes are preferred to continuous ones, such as the extrusion foaming. These techniques allow to evaluate in the most effective way the effects of polymer/gas mixture properties (such as viscosity, glass transition temperature, surface tension, gas solubility, and diffusivity) and processing parameters (temperature, pressure drop rate, and gas content) on cellular morphology and

density of foams, thanks to their ability to independently control the gas sorption step and the foaming step (cell nucleation and growth). Among all discontinuous foaming techniques, we have used the batch foaming[11,12] and the solid-state[3,10] techniques. In the first case, cell nucleation was promoted by controlling the pressure drop rate directly in the pressurized vessel used to solubilize the blowing agent. In the solid-state process, foaming was promoted by increasing the temperature of gas-saturated samples in an oil bath after the blowing agent solubilization.

Some authors have already used the solid-state method to investigate the properties of some engineering thermoplastic polymers.[2,13–18] They put in evidence that foaming only takes place in the temperature range between the T_g of the polymer/gas mixture and an upper bound temperature, T_{upper}. Their results suggested that the dominating factor controlling the foaming process was the ability of the blowing agent (CO_2) to plasticize the polymer matrix. According to Tang et al.,[19] high carbon dioxide content could result in a blowing agent gradient along the sample thickness. This aspect could heavily influence the final morphology of such thermoplastic polymers.

Most of the previous works on high-performance foams were predominantly focused on amorphous matrices but, among the semicrystalline polymers, foaming of PET and PEEK was also investigated.[5,11,18,20]

The goal of this paper was to investigate the foaming process of several amorphous engineering thermoplastic polymers (polyethersulfone, PES; polyphenylsulfone, PPSU; polyetherimide, PEI) and of a semicrystalline one (PEN). The latter was selected because of its lower processing temperatures when compared to PEEK, PEK, and PEKK. In fact, it possesses a high T_g (125°C, only 20°C lower than T_g of PEEK) with the advantage of a melting temperature of 260°C, allowing less difficult processing conditions.

Experimental

The polymers used (PES, Ultrason E3010 from BASF, Ludwigshafen, Germany; PPSU, Radel R5000 from Solvay, Brussels, Belgium; PEI, Ultem 1000 from General Electric, Fairfield, CT; PEN, Teonex TN8065S from Teijin, Osaka, Japan) were selected according to the requirement of a minimum continuous working temperature of 200°C.

The blowing agent, carbon dioxide with a purity of 99.9%, supplied by S.O.N. (Società Ossigeno Napoli, Italy), was used as received. The polymers were vacuum dried at 120°C for 24 h before all the tests (thermal and rheological analysis, gas sorption, and foaming processes).

Thermal properties were evaluated by using a differential scanning calorimeter (Q1000 DSC from TA Instruments, New Castle, DE). The glass transition (T_g) and melting (T_m) temperatures were determined by means of a heating scan from room temperature to 300°C at a heating rate of 10°C/min. The maximum crystallinity of PEN was evaluated after complete crystallization and reported. Nonisothermal crystallization kinetics was qualitatively evaluated by performing DSC cooling tests from the melt state, with cooling rates ranging from 1 to 10°C/min.

Rheological oscillatory tests were conducted by using a parallel plate rheometer (ARES from Rheometric Scientific, now TA Instruments, New Castle, DE). Amorphous polymers were tested between 320°C and 380°C, whereas semicrystalline polymers were tested between 240°C and 300°C. The complex viscosity was evaluated in the frequency range between 0.1 and 10 Hz, and master curves at 340°C for amorphous and at 240°C for semicrystalline polymers were calculated.

Sorption measurements were performed to evaluate the solubility of CO_2 in the selected polymers. The solubilization of carbon dioxide was performed in a pressure vessel at 50°C and 65 bar, and the gas uptake was measured after 24, 48, and 72 h by means of a high precision balance. The absorbed CO_2 was measured as a difference between the weight after the selected sorption time in the high-pressure vessel and that of the dried sample. The weight of more than five samples for each polymer was used to evaluate the average CO_2 sorption value. The time delay between the sample extraction from the sorption vessel and the sample weighting was lower than 10 s.

Samples for the foaming process were prepared in the form of 0.5-mm thick sheets by the compression molding technique and then quenched from the melt state to assure the complete amorphous state before the gas solubilization step.

Two different techniques were used to foam the samples: the solid-state and the batch-foaming processes. In the first method, the polymers were vacuum dried at 120°C for 24 h and then saturated for 48 h in a pressure vessel with CO_2 at a pressure of 65 bar and a temperature of 50°C. Subsequently, the saturated samples were taken out from the vessel and dipped in an oil bath kept at the desired

TABLE I
Material Properties

Polymer	T_g (°C)	T_m (°C)	Density (g/cm^3)	ΔH_m (J/g)	X_c (%)
PES	225	–	1.37	–	–
PPSU	220	–	1.29	–	–
PEI	215	–	1.28	–	–
PEN	125	260	1.33	56.7	30

Relative crystallinity was evaluated considering ΔH_m^o from Ref. 22.

temperature. The temperature range for the solid-state foaming process was 160–240°C for both amorphous and semicrystalline polymers.

For the batch-foaming technique, the samples were saturated with CO_2 in the same conditions as for the solid-state method, but after 48 h they were heated to the desired temperature directly in the high-pressure vessel. As the target temperature was reached, the internal pressure was suddenly dropped to the atmospheric pressure at a pressure drop rate of 40 MPa/s. In this case, the temperatures investigated were 140–260°C for amorphous polymers and 100–260°C for semicrystalline polymers. It is worth to note that only results regarding foams with good cellular structure are reported and discussed below.

The relative density of foams was calculated as the ratio between the foam density ρ_f (measured by the water-displacement method according to ASTM D792 standard) and the polymer bulk density. Because of the integral skin and closed-cell structure of all samples prepared, no water uptake was detected during measurements.

The morphological parameters of the cellular structures were evaluated from SEM micrographs (SEM S440 from Leica Microsystems, Wetzlar, Germany). In particular, the mean cell diameter was calculated from, at least, 50 measures, whereas the cell density N_0 (the number of cells nucleated per unit volume of the original unfoamed polymer) was calculated with the following formula[21]:

$$N_0 = \left(\frac{n}{A}\right)^{\frac{3}{2}} \frac{1}{1 - V_f} \quad (1)$$

with

$$V_f = 1 - \frac{\rho_f}{\rho_s} \quad (2)$$

where V_f is the void fraction of foam, ρ_f is the foam density, ρ_s is the bulk polymer density, n is the number of cells in the SEM micrograph, and A is the area of the micrograph in cm^2.

Results and Discussion

Thermal and rheological properties of the polymeric matrices were evaluated because of their role in the foaming process. In particular, the glass transition (T_g) and melting (T_m) temperatures measured on the selected polymers (Table I) by means of DSC analysis were performed to evaluate the foaming temperature range for both foaming techniques. All the amorphous polymers clearly exhibited a glass transition temperature well above 200°C.

PEN showed a maximum crystallinity of 30% and was able to crystallize only when slow cooling rates were employed (Fig. 1); therefore, the crystallinity of PEN samples was very low, except at a cooling rate of 1°C/min, as shown in Table II. During the

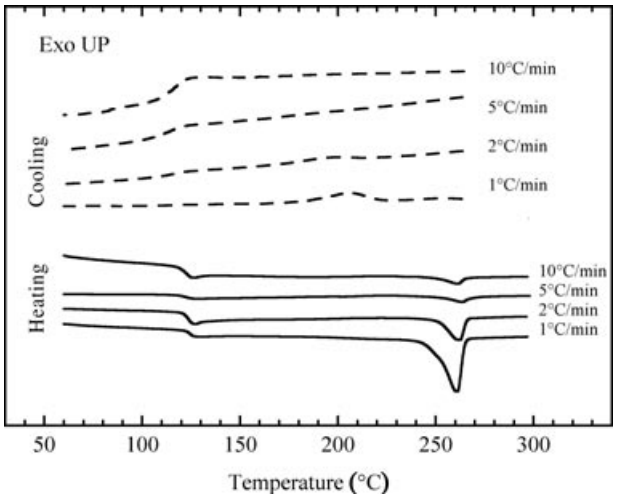

FIGURE 1. DSC analysis of PEN at different cooling rates.

TABLE II
Thermal Properties from Dynamic DSC Scans of PEN Polymer

Cooling			Heating		
Cooling Rate (°C/min)	X_c (%)	Peak T_c (°C)	Heating Rate (°C/min)	X_c (%)	Peak T_m (°C)
1	9.84	205.75	10	1.47	260.62
2	3.26	195.26	10	0.25	262.28
5	2.21	225.32	10	0.63	263.62

Relative crystallinity was evaluated considering ΔH_m^o from Ref. 22.

second heating scan, further but small crystallization occurred.

The master curves of the complex viscosity of the polymeric matrices evaluated at about 120°C above their glass transition temperatures (240°C for PEN and 340°C for PEI, PPSU, and PES) are shown in Fig. 2. The complex viscosities of all polymers were not much different in these conditions, even if the PEN matrix exhibited a slightly lower viscosity when compared to the others polymers. The complex viscosity of PEN ranged from 5×10^3 Pa s at low strain rates to 1.3×10^3 Pa s at high strain rates. Among the amorphous polymers, PES showed the lowest viscosity, ranging from 6×10^3 at 10^{-2}Hz to 3×10^3 at 10 Hz.

It is worth to outline that the measurement of the complex viscosity of the semicrystalline PEN matrix at a temperature ($T = 240$°C) lower than T_m was possible, because of the low crystallization kinetics, as previously discussed.

The CO_2 uptake as a function of the sorption time for the different polymers is reported in Fig. 3. Most of the gas uptake in the selected polymers was reached after 48 h with only a slight increase at 72 h. Although PEN samples were in the amorphous state, since they were quenched from the melt state before sorption measurements, it is interesting to observe that the CO_2 uptake after 48 h was about one-half of the amorphous polymers.

The morphologies of the foam samples prepared with the solid-state process are shown in Fig. 4. The relative densities, plotted as a function of the foaming temperature in Fig. 5, show that the semicrystalline PEN matrix exhibited the highest expansion ratios and that all amorphous polymers did not show cell nucleation below 180°C.

Relative densities between 0.13 and 0.44 were obtained with PEN in a wide range of temperatures (from 160°C to 240°C), whereas, by using the solid-state foaming technique, relative foam densities

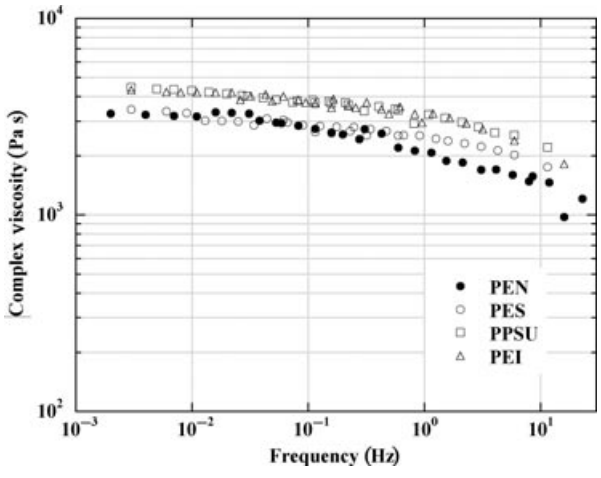

FIGURE 2. Master curves of complex viscosity for all polymers.

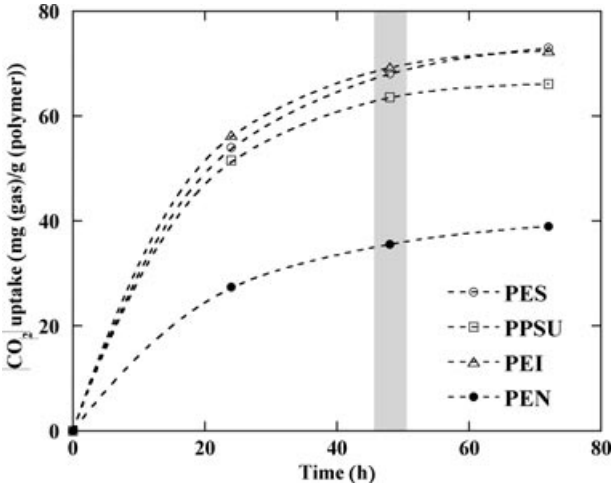

FIGURE 3. Sorption of carbon dioxide at 50°C and 65 bar.

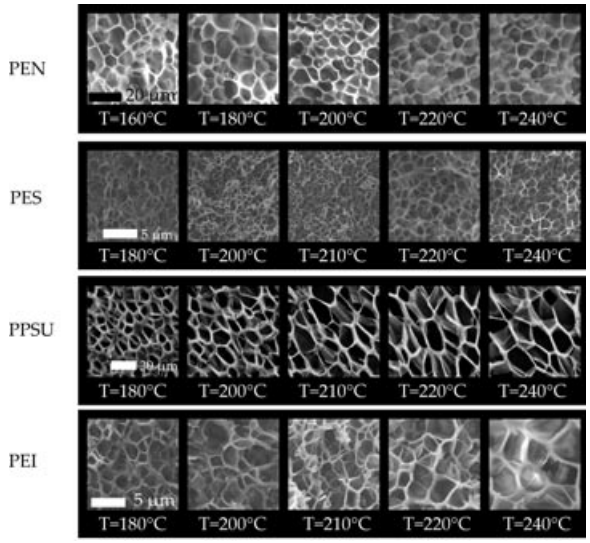

FIGURE 4. SEM micrographs of foams prepared with the solid-state foaming process at different temperatures.

obtained from PES, PEI, and PPSU ranged between 0.25 and 0.6 (from 180°C to 240°C). PEI and PES exhibited a minimum of the relative density in the explored temperature range. In particular, PEI showed the minimum relative density at a temperature around its bulk T_g, whereas PEN foams showed a minimum at a temperature 80°C higher than its T_g. The minimum relative density of PEI was 0.25, two times higher than the minimum value of PEN, and was in contrast with the amount of gas solubilized in

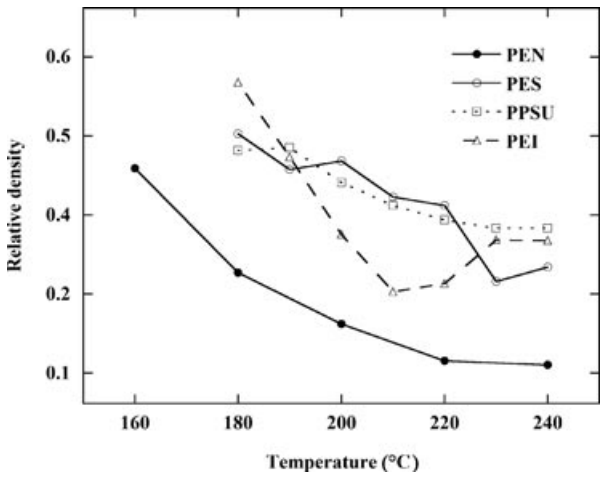

FIGURE 5. Relative densities of polymers as a function of the foaming temperature for the solid-state process.

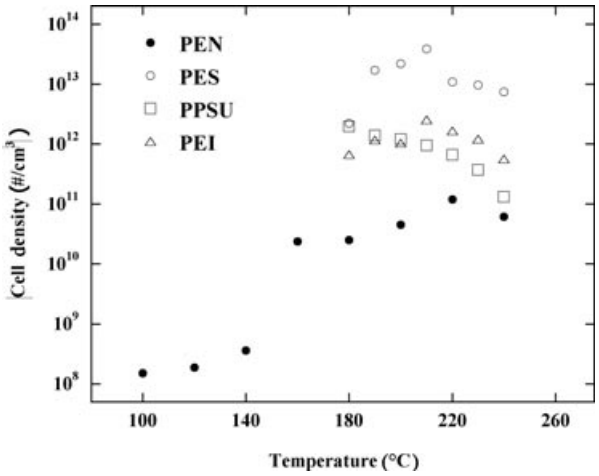

FIGURE 6. Cell densities of foams prepared by means of the solid-state process.

the different polymers. As a result, the relative densities of PEI, PPSU, and PEI foams were significantly higher than those exhibited by the semicrystalline polymer for each foaming temperature.

The cells density of all samples prepared with the solid-state foaming technique is shown in Fig. 6. PEN was characterized by lower N_0 values (ranging from 10^8 to 10^{11}) when compared to all amorphous polymers (N_0 ranging from 10^{11} to 10^{14}). In particular, when the foaming temperature was lower than the T_g, N_0 values for PEN drastically dropped of two order of magnitude. An opposite behavior was exhibited by the amorphous polymers, whose foams presented a high number of cells (especially for PES) with low diameters, nucleated at all foaming temperatures either below or above the bulk polymer T_g. As the foaming temperature approached the neat polymer T_g from 240°C, N_0 raised up to a maximum then decreased (except that for PPSU, which exhibited a monotonic increasing trend) and cell diameters decreased.

The different behaviors were attributed to the different conditions in which the foaming process took place with respect to the glass transition temperature of the gas/polymer mixture. It should be noted that PEI, PPSU, and PES were foamed in a temperature range starting well below their bulk T_g, and very good results were obtained, especially in terms of the high number of nucleated cells. Foams from PEN were obtained only at temperatures well higher than its T_g (starting from 160°C, Fig. 5). This clearly indicated that the glass transition temperature T_{gm} of the gas/polymer mixture for amorphous polymers

was lower than the foaming temperature (from 180°C).

Equation (1), from the classic theory of bubble foaming [rearranged from Ref. 23], relates the nucleation rate J to the processing conditions of the foaming process:

$$J = [M][B]\exp\left(-\frac{\Delta G_c}{kT}\right) \tag{3}$$

where M is a factor related to the gas concentration, B is a frequency factor related to the diffusivity of the gas/polymer mixture, ΔG_c is the barrier energy for the formation of the stable nucleus of the bubble, k is the Boltzman constant, and T is the temperature.

The higher amount of solubilized blowing agent, affecting the M factor, was not enough to explain the very large number of nucleated cells in the amorphous polymers. In fact, as already discussed by other authors,[16,24] the other (and main, according to the authors) factor affecting the nucleation was the strong plasticization effect caused by a higher CO_2 content in the selected amorphous matrices. The CO_2 uptake influenced (a) the time scale of gas diffusion from the gas/polymer mixture to the cells and to the outside (raising the B factor through the glass transition temperature depression) and (b) lowered the barrier energy for the formation of the critical nuclei (lowering the ΔG_c). Higher gas content in the polymer depressed to a larger extent the glass transition temperature T_{gm} of the gas/polymer mixture and, as a consequence, the driving force for nucleation was higher at each foaming temperature T_f ($T_f > T_{gm}$). The T_{gm} of the gas/polymer mixture very quickly rose during the foaming process because of the gas escape from the polymeric matrix into the cells and consequently the mixture viscosity sharply and quickly increased. As long as the gas/polymer mixture T_{gm} was much lower than the foaming temperature, cells were able to nucleate but the raising viscosity hindered the cell expansion giving low cell diameters and high relative densities.

PEN samples were not able to be foamed when the foaming temperature was below or slightly above their T_g (Fig. 6). In these conditions, both the expansion and the cellular morphology were quite poor. The lower amount of solubilized gas resulted in a much lower plasticization of the polymeric matrix and, as a consequence, a higher polymer viscosity and a lower thermodynamical instability for foaming were exhibited. Further investigations should be performed to clearly clarify this phenomenon.

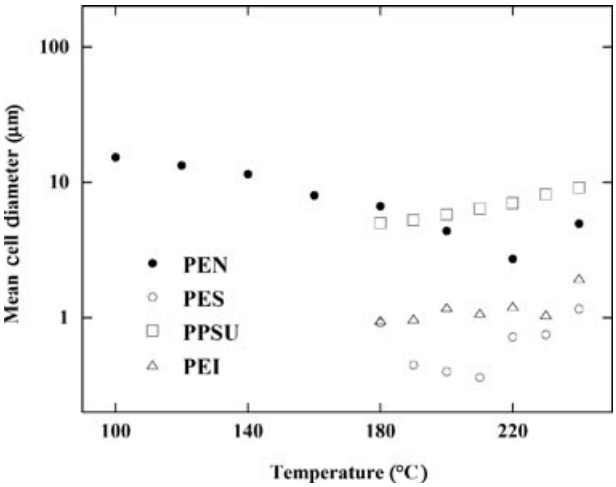

FIGURE 7. Mean cell diameters for foams obtained by means of the solid-state process.

The cellular morphology of all polymers, shown in Fig. 4, was microcellular. Cell diameters (Fig. 7) of semicrystalline samples were slightly decreased with the temperature up to a minimum, at 210°C. Amorphous polymers showed mean cell diameters growing with the foaming temperature because of the viscosity reduction with the temperature. In the temperature range between 170 and 240°C, PES samples exhibited a submicrocellular morphology and cells characterized by diameters of few hundred nanometers and nanoporous walls were widely detected, in particular at the highest foaming temperature investigated (Fig. 8). These structures are probably due to the fast decrease in the CO_2 concentration caused by the temperature, which escapes from the polymeric matrix to form the gaseous phase in a very fast manner. However, more work should be done to clearly understand this phenomenon but it is out of the scope of this paper.

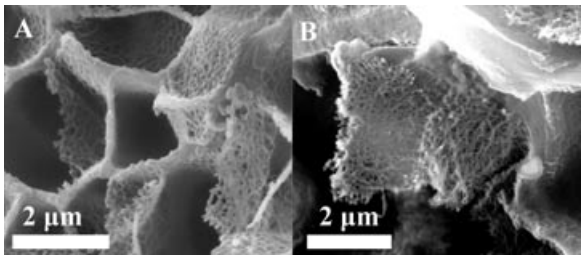

FIGURE 8. SEM micrographs of PES and PEI foams showing the sub-microcellular structures with nanoporous walls produced at 240°C.

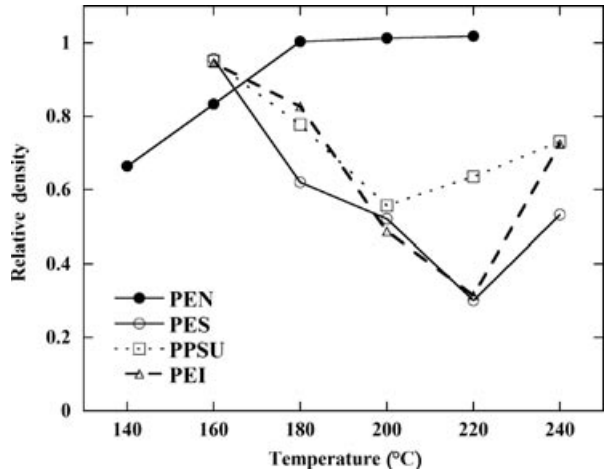

FIGURE 9. Relative densities of all polymers as a function of foaming temperature for the batch foaming process.

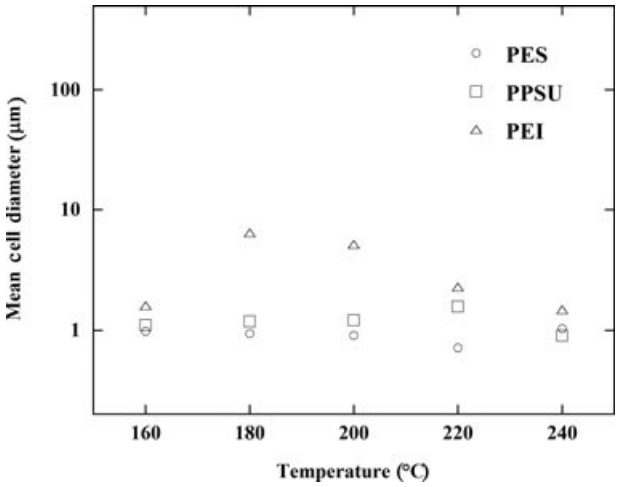

FIGURE 11. Mean cell diameters for foams obtained by means of the batch foaming process.

Relative density of samples produced by batch foaming was higher than that of foams prepared through solid-state process (Fig. 9), and the temperature ranges of latter process were narrower; in particular PEN foams presented very high relative densities.

The trend of both cellular morphologies (Fig. 10) and mean cell diameters (Fig. 11) proves that the dependence of the mean cell diameter on the foaming temperature was weak in the batch-foaming process, being cell dimensions quite constant for PES and PPSU and slightly decreased for PEI at higher temperatures. At 160°C, all amorphous polymers showed small but few nucleated cells, as a consequence of the very high polymer viscosity that hindered the cellular growth. Microcellular morphologies developed exclusively in PES, PPSU, and PEI, whereas few and very large cells were present in foamed PEN samples.

As evident from Fig. 12, the N_0 values of amorphous polymers produced by batch foaming were

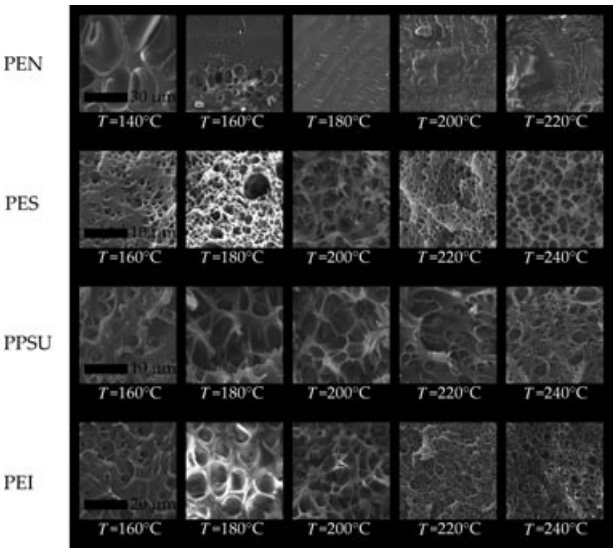

FIGURE 10. SEM micrographs of foams prepared with the batch foaming process.

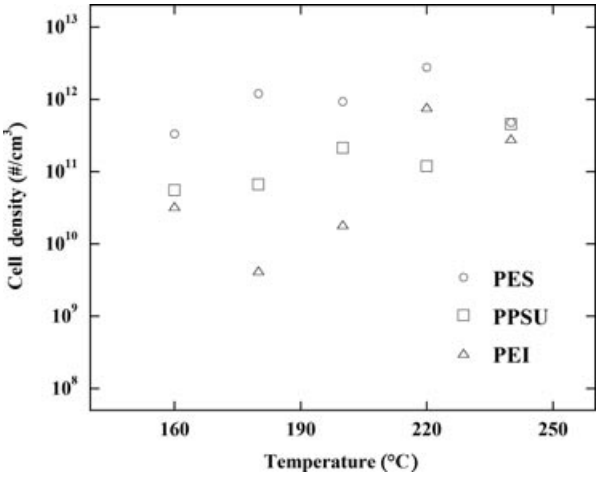

FIGURE 12. Cell densities of foams prepared by means of the batch foaming process.

TABLE III
Thermal Properties from DSC Scans on PEN Samples Foamed with the Solid State (SSF) and Batch-Foaming Techniques

	X_c (%)	
T_{foam} (°C)	SSF	BATCH
120	5.1	–
140	9.8	–
160	11.5	18.9
200	5.2	15.6
220	–	22.2
240	6.4	18.3

Relative crystallinity was evaluated considering ΔH_m^o from Ref. 22.

two order of magnitude lower than in the case of solid-state foaming technique at the same foaming temperatures. PEN samples exhibited irregular morphologies at 160 and 180°C and were not foamed at higher temperatures. It is interesting to note that cell density of amorphous polymers prepared by batch foaming slightly increased with the temperature unlike foams produced by solid-state technique (Fig. 6).

The temperature played a very important role in the batch-foaming process, being responsible for (a) the gas desorption from the polymeric matrix during the heating step (see the Experimental section) and (b) the crystallization of the PEN matrix. The reduction in gas solubility was the main factor, affecting the foaming process of amorphous polymers. In fact, the lower amount of solubilized gas resulted in a combined effect of lower T_g depression and lower thermodynamical instability (driving force) that leaded to reduced cell density with respect to the solid-state foams. Furthermore, the relative densities were higher when compared to the solid-state foaming samples, because of the lower amount of absorbed gas and the temperature range for foaming was narrowed and shifted toward higher temperatures.

On the contrary, the crystallization was the main factor affecting the foaming process of the PEN matrix. In this case, a quite complete crystallization of the macromolecules occurred during the heating step from the sorption temperature to the foaming temperature (Table III). Cell nucleation and growth could not take place due to the higher crystallinity of the PEN samples.

It should be noted that the characteristic time of the solid-state foaming process (few seconds) was much lower than the time needed to crystallize the PEN matrix, because the time interval during the temperature raise, by immersing the samples in the oil bath, was quite instantaneous and low crystallinity was developed (Table III). On the contrary, the heating step in the batch-foaming process was of several minutes and during this time the PEN crystallized (Table III). Few sparse cells were nucleated, and they grew only when the lowest foaming temperatures were used.

Conclusions

Foams from high-performance thermoplastic polymers (PEN, PES, PEI, and PPSU) were prepared by using two different foaming techniques, namely solid state and batch foaming, and carbon dioxide as a blowing agent.

PEN foams exhibited the lowest relative densities (the minimum value was 0.13) and the widest temperature window for foaming among all samples prepared by the solid-state foaming technique. Conversely, the amorphous polymers presented the highest cell densities and the smallest cell diameters (less than 1 μm in some conditions for PES).

Amorphous matrices always showed microcellular morphology at foaming temperatures either below or above the bulk polymer glass transition temperature (T_g) due to glass transition temperature (T_{gm}) lowering of the gas/polymer mixture induced by the higher amount of solubilized CO_2. In some processing conditions, PES and PEI samples exhibited nanoporous cell walls and submicrocellular average diameters of cells. The lower amount of absorbed gas in PEN hindered the formation of regular morphology at foaming temperatures below T_g. Furthermore, in solid-state foaming the gas/polymer demixing during the gas escaping from the polymeric matrix, particularly fast in amorphous polymers, prevented high expansion ratios but allowed both quenching of the cellular structure and very high cell densities. PEN foams showed lower cell densities in all processing conditions.

When the batch-foaming process was used, the gas loss from polymeric matrices occurring in the heating step, resulted in an increase in the foam density and the temperature range of foaming process was reduced and shifted toward higher temperatures for all matrices with respect to the solid-state foaming technique. Even in batch-foaming process, amorphous matrices showed microcellular

morphology but the number of nucleated cells was lower than in the solid-state foaming process.

The crystalline phase developed in most PEN samples during heating; its formation was facilitated by the solubilized carbon dioxide in the matrix and prevented a regular cellular structure organization.

Acknowledgments

The authors would like to thank Vincenzo Scognamiglio for the contribution to all experimental activities.

References

1. Gibson, L. J.; Ashby, M. F. Cellular Solids: Structure and Properties, 2nd ed.; Cambridge University Press: Cambridge, UK, 1997.
2. Mascia, L.; Del Re, G.; Ponti, P. P.; Bologna, S.; Di Giacomo, G.; Haworth, B. Adv Polym Technol 2006, 25(4), 225–235.
3. Hongliu, S.; Mark, J. E. J Appl Polym Sci 2002, 86, 1692–1701.
4. Hongliu, S.; Sur, G. S.; Mark, J. E. Eur Polym J 2002, 38, 2373–2381.
5. Sorrentino, L.; Di Maio, E.; Iannace, S. J Appl Polym Sci 2010, 116(1), 27–35.
6. Colton, J. S.; Suh, N. P. Mater Manuf Process 1986, 1(3–4), 341–364.
7. Jonathan, S.; Colton, J. S.; Suh, N. P. Polym Eng Sci 1987, 27(7), 500–503.
8. Yamaguchi, H.; Yamamoto, S. U.S. Patent 6576683, 2003
9. Alcan Composites (Switzerland), Airex C71 datasheet.
10. Klempner, D.; Sendjarevic, V. Polymeric Foams and Foam Technology, 2nd ed.; Hanser Publishers: New York, 2000.
11. Reverchon, E.; Cardea, S. Supercrit Fluids 2007, 40(1), 144–152.
12. Di Maio, E.; Mensitieri, G.; Iannace, S.; Nicolais, L.; Li, W.; Flumerfelt, R. W. Polym Eng Sci 2005, 45(3), 432–441.
13. Krause, B.; Boerrigter, M. E.; van der Vegt, N. F. A.; Strathmann, H.; Wessling, M. J Membr Sci 2001, 187, 181–192.
14. Krause, B.; Van Der Vegt, N. F. A.; Wessling, M. Desalination 2002, 144(1–3), 5–7.
15. Krause, B.; Diekmann, K.; Van DerVegt, N. F. A.; Wessling, M. Macromolecules 2002, 35, 1738–1745.
16. Krause, B.; Sijbesma, H. J. P.; Munuklu, P.; van der Vegt, N. F. A.; Wessling, M. Macromolecules 2001, 34, 8792–8801.
17. Krause, B.; Mettinkhof, R.; van der Vegt, N. F. A.; Wessling, M. Macromolecules 2001, 34, 874–884.
18. Dong, W.; Wei, J.; Hong, G. J Appl Polym Sci 2009, 111(4), 2116–2126.
19. Muoi, T., Yi-Ching, H., Yan-Ping, C. J Appl Polym Sci 2004, 94(2), 474–482.
20. Brolly, J. B.; Bower, D. I.; Ward, I. M. J Polym Sci, Part B 1996, 34, 769–780.
21. Gosselin, R.; Rodrigue, D. Polym Test 2005, 24, 1027–1035.
22. Buchner, S.; Wiswe, D.; Zachmann, H. G. Polymer 1989, 30, 480–488.
23. Gibbs, W. The Scientific Papers, Vol. 1; Dover: New York, 1961.
24. Chen, X.; Feng, J. J.; Bertelo, C. A. Polym Eng Sci 2006, 46(1), 97–107.